CHROM. 4435

BAND SPREADING IN MOLECULAR-SIEVE CHROMATOGRAPHY

NEALE POVEY* AND ROBERT A. HOLM
The Institute of Paper Chemistry, Appleton, Wisc. 54911 (U.S.A.)

(Received August 22nd, 1969)

SUMMARY

Band spreading was studied in aqueous molecular-sieve chromatography systems using carbohydrate solutes. Bio-Gel P-2, Sephadex G-10, and Sephadex G-15 were used. P-2 gel was prepared in three size fractions by wet screening and elutriation. All gel preparations were characterized by extensive size measurements with a digital coding microcomparator. The band spreading behavior of solutes followed a theory based on the additivity of the mechanisms of axial dispersion and slow mass transfer. The molecular diffusion of solute in the gel phase was found to be the controlling mechanism of mass transfer (with substances of low molecular weight). A diameter equivalent to the most probable spherical volume was used in describing slow gel phase diffusion. Using the random walk theory of eddy diffusion, it was found that a diameter equivalent to the most probable specific area of the particles was best to describe axial dispersion.

INTRODUCTION

In all types of chromatography, band spreading is present and detracts from the efficiency of the separation process. Polymer applications of molecular-sieve chromatography (MSC) endeavor to order a disperse molecular weight preparation. The resulting chromatograms show the distribution of molecular weights as modified by band spreading. Other applications of MSC include the separation of solutes into semi-pure fractions. In these operations, band spreading leads to overlapping or cross-contamination of solutes. In both types of MSC operation, the mechanisms leading to band spreading are analogous if not identical.

The first theories of chromatography were descriptive, based on distillation plate models[1,2]. Later, by considering a continuously flowing system, it was possible to incorporate operating parameters such as particle diameter and eluent flow rate[3,4].

* A portion of a thesis submitted by NEALE POVEY in partial fulfillment of the requirements of The Institute of Paper Chemistry for the degree of Doctor of Philosophy from Lawrence University, Appleton, Wisc.; January, 1969.

The most recent theoretical approaches to the mechanisms of band spreading in MSC include coupling[5], flow profile[6], and diffusion-controlled partitioning[7].

The theory used with this work is based on previous developments of HAMILTON *et al.* concerning the behavior of ion-exchange systems[8]. Assuming that axial dispersion and mass-transfer effects can be combined linearly, eqn. (1) was derived[9]

$$H\alpha = \frac{2\,D_{ax}}{U} + \frac{2\,K_1^2\,\varepsilon U}{(K_1 + \varepsilon)^2\,K_L} \tag{1}$$

Assuming that slow gel-phase diffusion-controlled mass-transfer resistance, eqn. (2) was derived[9].

$$H\alpha = 2\,\lambda d_p + \frac{K_1\,\varepsilon}{(K_1 + \varepsilon)^2}\,\frac{d_p^2}{30\,D_g}\,U \tag{2}$$

where H = height of an equivalent theoretical plate, U = interstitial fluid velocity, D_g = gel-phase diffusion coefficient, D_{ax} = effective axial diffusivity, K_1 = distribution coefficient, d_p = diameter of a monodisperse gel fraction, ε = packing porosity, λ = 'eddy diffusion' coefficient, K_L = overall mass-transfer coefficient. The distribution coefficient is defined as

$$K_1 = \frac{V_e - V_0}{V_t}$$

where V_e = elution volume, V_0 = void volume, and V_t = total volume. The variable α is defined as

$$\alpha = \sqrt{1 - \frac{2}{N}} \tag{3}$$

where N = number of theoretical plates. This term was included because the extended plate theory of GLUECKAUF[3] was used in the derivations instead of the simpler theory of MARTIN AND SYNGE[1]. The factor α allows correct calculations to be made in relatively inefficient MSC systems, *ca.* less than 200 theoretical plates.

EXPERIMENTAL

One kilogram of 50–100 mesh Bio-Gel P-2 was fractionated in a Bauer-McNett fiber classifier. Three of the standard screen fractions were further fractionated in a 6 × 40 cm elutriation column. Ungraded Sephadex G-10 and G-15 gels were fractionated by repeated sedimentation and siphoning.

Gel hydration parameters

The water regain of the gels was measured by a method which combines filtration and vacuum distillation. The P-2 gel was also characterized by a method which measures the increased concentration of an excluded solute when the dry gel is swollen. The gel was swollen in an aqueous solution of a high polymer.

Dental dam method. Common filtration and centrifugation methods of measuring water regain do not satisfactorily account for pore water. This has been discussed by PEPPER *et al.*[10]. To circumvent this, all of the pore water was removed by vapor transport.

A quantity of dry gel was weighed and swollen to equilibrium in water. The

hydrated gel was then washed into a coarse, sintered-glass filter crucible. The bulk of the pore water was removed with suction; then a piece of dental dam was fastened over the crucible and the filtration continued for 20 min. The filter and contents were weighed, and the water regain was calculated using the equation

$$w_r = \frac{\text{wet gel (g)} - \text{dry gel (g)}}{\text{dry gel (g)}} = \frac{\text{hydration water (g)}}{\text{dry gel (g)}} \quad (4)$$

The dental dam served as a flexible barrier, making the entire gel sample subject to vacuum. As shown in Fig. 1, a definite change in the rate of water removal occurred after 20 min. It was inferred from this behavior that pore water was first removed, followed by hydration water. In applying this method to other materials, the weight loss *versus* time behavior must first be studied to ascertain the proper length of filtration.

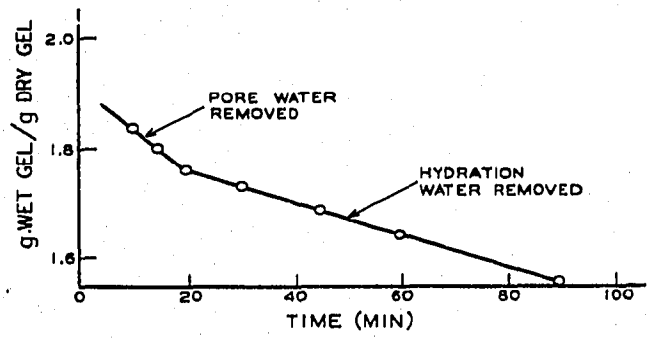

Fig. 1. Water loss during dental dam filtration of hydrated P-2 gel.

Data shown in Table I are an average of five determinations.

TABLE I

WATER REGAIN DATA

	w_r (g/g)	*Average deviation* (g/g)
Bio-Gel P-2 (excluded solute)	1.40	0.04
Bio-Gel P-2 (dental dam)	1.38	0.04
Sephadex G-15 (dental dam)	1.21	0.03
Sephadex G-10 (dental dam)	0.79	0.02

Excluded solute method. Through a simple mass balance, the following equation relating water regain to measurable parameters can be derived:

$$w_r = \frac{V_s \varrho \, (1 - c_0/c)}{M_{gel}} \quad (5)$$

where w_r = water regain, V_s = volume of solution initially added to dry gel, ϱ = density of solution, M_{gel} = mass of dry gel, c_0 = initial concentration of excluded solute, c = final concentration in interstitial fluid.

The results shown in Table I were obtained from five samples of ungraded Bio-Gel P-2. The solution was a preparation of Sephadex brand Blue Dextran 2000 at an initial concentration of about 375 μg/ml. The gel was removed from the interstitial fluid with a syringe filter, adding the solution directly to the spectrophotometer cells. The initial and final concentrations were determined from an absorbance calibration plot at 600 nm.

Specific volumes

The wet and dry specific volumes of the gel particles are defined as

$$\bar{V}_w = \frac{\text{volume of hydrated gel (ml)}}{\text{dry gel (g)}} \tag{6}$$

and

$$\bar{V}_d = \frac{\text{volume of dry gel (ml)}}{\text{dry gel (g)}} \tag{7}$$

These specific volumes can be used to calculate a useful parameter, the gel porosity, defined as

$$\varepsilon_g = \frac{\text{hydrated volume of gel}}{\text{total volume of gel}} \tag{8}$$

Using the relationship

$$\varepsilon_g = 1 - \frac{\bar{V}_d}{\bar{V}_w} \tag{9}$$

the specific volumes were calculated from measurements of sedimented volumes in graduated cylinders. The wet volume was measured in water, and the dry volume was measured in absolute ethanol, a nonswelling solvent for the gels. The porosity of 0.47 for random loose arrangements of spheres[11] was used to calculate actual gel volumes from the observed sedimented volumes. Data shown in Table II are an average of seven determinations.

TABLE II

WET AND DRY SPECIFIC VOLUME

Gel	$\bar{V}_w$ (cm^3g^{-1})	*Average deviation*	$\bar{V}_d$ (cm^3g^{-1})	*Average deviation*	ε_g
P-2	2.01	0.023	0.994	0.008	0.506
G-10	1.21	0.006	0.952	0.023	0.215
G-15	1.63	0.011	0.869	0.011	0.466
G-25	2.47	0.020	0.663	0.005	0.731

Gel diameter measurements

About 1500 diameters were measured from each of three P-2 gel preparations and about 1000 from the G-10 and G-15 preparations. Measurements were made with a digital coding microcomparator coupled with a data card punch. The data were compiled through the computer facilities at The Institute of Paper Chemistry. The

gel preparations were characterized by the various averages shown in Table V and additional distribution parameters which have been discussed elsewhere[9].

Solutes

The solutes were commercial preparations, purified by filtering the solutions with Darco G-60 activated carbon. Information pertinent to the solutes is given in Table III.

TABLE III

SOLUTES

Solute	*Abbreviation*	*Molecular weight*	*Diffusion coefficient, D_m (25°, H_2O, $cm^2sec^{-1} \times 10^6$)*
Glycine	GY	75	10.64
Glycerin	GC	95	9.4
Glucose	GLC	180	6.73
Sucrose	SUC	342	5.21
Raffinose	RAF	504	4.34
Schardinger α-dextrin	SAD	972	3.44
Schardinger β-dextrin	SBD	1,134	3.22
Sephadex brand Dextran 10	DEX	12,000	1.095

Chromatographic system

The equipment used in the experimental measurement of band spreading is shown in Fig. 2. The deaerator consisted of a heater and a bubble collector constructed

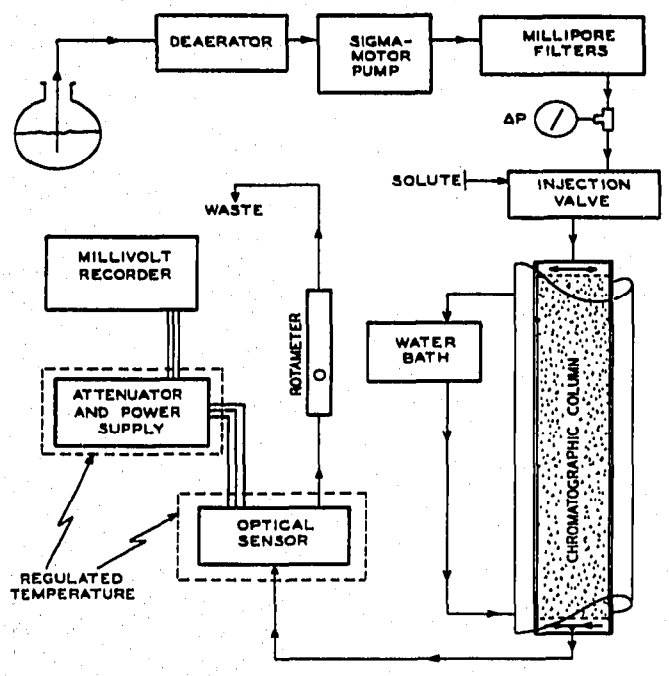

Fig. 2. Experimental chromatographic system.

from glass. A Sigmamotor Series T-8 pump was used with a duplex manifold of 3/16-in. O.D. Tygon tubing, formulation S 50 HL. Two Millipore filters were used, 8 μm and 3 μm. The injector valve was Chromatronix Model SV-8031 and the column was Chromatronix Model LC-1, a 1 × 20 in. column equipped with a water jacket. The detector was the Nestor/Faust Model 404 R.I. monitor. The optical head was packed with 200-μm glass beads to improve the dynamic response. Both the optical head and the power supply were temperature controlled to assure a steady base line.

The column was repacked between most of the temperature changes. This was done by filling the column with water and adding the gel as a slurry to a large funnel attached to the top of the column. In all of the major data runs, samples of 0.5 ml solution were used. Most solutes were injected at 5–7% concentrations (w/v). Dextran was used at 1–2%. The concentration of Schardinger β-dextrin was limited by its solubility, *ca.* 3%.

DATA REDUCTION

The height equivalent of a theoretical plate (HETP) of each curve was calculated from GLUECKAUF's equations[12].

$$N = \frac{8\,V_e\,(V_e - W_1)}{(W_1 + W_2)^2} \tag{10}$$

$$L' = L - \frac{V_f}{2A\varepsilon} \tag{11}$$

$$H = N/L' \tag{12}$$

where N = number of theoretical plates, V_e = corrected elution volume, L = measured length of packing, L' = corrected length, V_f = sample volume, ε = porosity, A = cross-sectional column area, and W_1 and W_2 are the leading and trailing widths of the elution curve measured at h/e.

Four to ten flow rates were used in the data runs, ranging from 0.15 to 5.0 ml/min. The data pertinent to each elution curve were recorded on punched cards and the analysis was made through computer programs. All the runs gave linear H or $H\alpha$ *versus* U plots as shown for the representative data in Fig. 3. The average correlation coefficient of all runs was 0.996. The slope and intercept were calculated from a least-squares analysis and these were used to calculate the following quantities:

$$\text{intercept} = H_0 \tag{13}$$

$$\frac{1}{K_L} = \frac{m\,V_0}{2\,V_t}\left(\frac{V_e - V_0}{V_e}\right)^2 \tag{14}$$

$$D_g = \frac{d_p^2\,V_0\,(V_e - V_0)}{30\,m\,V_e^2} \tag{15}$$

where d_p = particle diameter, V_e = peak elution volume, V_0 = void volume, V_t = total column volume, and m = the slope of the experimental $H\alpha$ *versus* U plot.

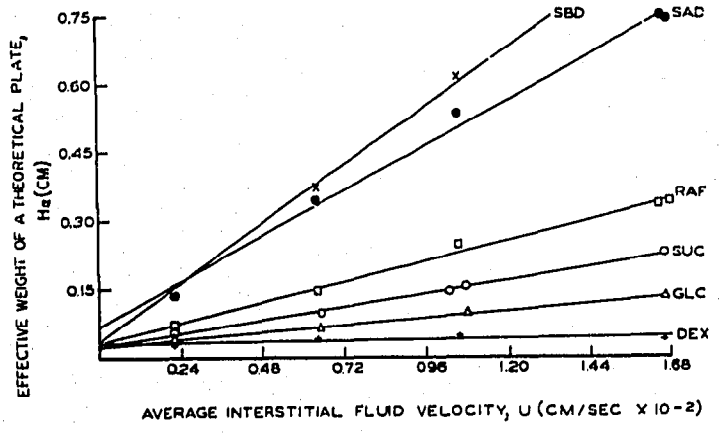

Fig. 3. Representative *Ha versus U* plot. (See Table III for abbreviations.).

RESULTS

Reproducibility

The column was repacked and the conditions were repeated four times. As shown in Table IV, there was good agreement between m, K_1, and ε. The large amount of variation of the parameter H_0 reflects the sensitivity of axial dispersion to changes in packing structure. The reproducibility data indicate that mass transfer parameters can be compared between packings but that only the gross axial dispersion behavior can be evaluated.

TABLE IV

REPRODUCIBILITY OF COLUMN PARAMETERS

70–80 mesh Bio-Gel P-2, 45°. Average correlation coefficient = 0.993. m = slope of *Ha versus U* (sec^{-1}); H_0 = intercept of *Ha versus U* (cm).

Run	*Raffinose*			*Glucose*			
	m	H_0	K_1	m	H_0	K_1	ε
13	11.50	0.079	0.291	4.34	0.068	0.412	0.354
46	11.71	0.040	0.296	5.03	0.029	0.414	0.365
47	11.76	0.052	0.288	4.89	0.044	0.414	0.381
48	11.33	0.041	0.293	4.93	0.034	0.412	0.368
Mean	11.58	0.053	0.292	4.80	0.044	0.413	0.367
Av. dev.	0.16	0.013	0.005	0.23	0.012	0.001	0.007
% dev.	1.4	25	1.7	4.8	27	0.24	1.9

Diameter averages

The following equations define the averages which were calculated for the gel preparations:

$$d_{sps} = \left(N \sum^{N} \left(1/d_n\right)\right)^{-1} \tag{16}$$

$$d_n = \sum^{N} d_n/N \tag{17}$$

$$d_{sv} = \left(\sum^{N} d_n^3\right)^{\frac{1}{3}} \Big/ N$$

$$d_a = \sum^{N} d_n^3 \Big/ \sum^{N} d_n^2$$

$$d_{wv} = \sum^{N} d_n^4 \Big/ \sum^{N} d_n^3$$

The relationship between the averages is shown schematically in Fig. 4 for the fractionated P-2 gel preparations. Table V is a more detailed presentation of the diameter data. The relative uniformity of diameter within the fractionated samples can be inferred from the ratios of volumetric to linear average.

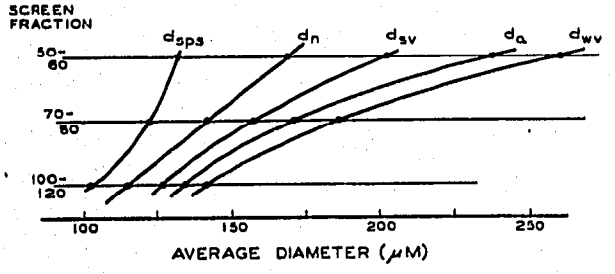

Fig. 4. Average diameters for fractionated gel.

TABLE V

DIAMETER AVERAGES

Preparation	d_{sps} (μm)	d_n (μm)	d_{sv} (μm)	d_a (μm)	d_{wv} (μm)
100–120, P-2	104.47	116.68	125.93	134.97	141.55
70–80, P-2	123.40	143.60	158.57	173.16	182.96
50–60, P-2	133.20	170.12	204.49	240.78	263.91
Sephadex G-10	72.48	76.06	79.77	83.61	87.38
Sephadex G-15	80.97	83.74	86.79	89.97	93.36

In order to ascertain the proper average for mass transfer, eqns. (1) and (2) were assumed to be exact. Values of K_L were calculated, and D_g was calculated using each of the averages. The experimental data were derived from band spreading measurements using three preparations of Bio-Gel P-2. Two solutes were used, glucose and raffinose; and runs were made at three temperatures, 15, 30, and 45°.

The deviations of D_g from group averages were used as one measure of the consistency of a diameter average. The deviations were normalized and combined until one value was obtained which was representative of the error associated with a given average. The results of this analysis are shown schematically in Fig. 5, abbreviated ΔD_g.

The overall mass transfer coefficient can be written

$$\log \frac{1}{K_L} = 2 \log d_p - \text{constant} \qquad (21)$$

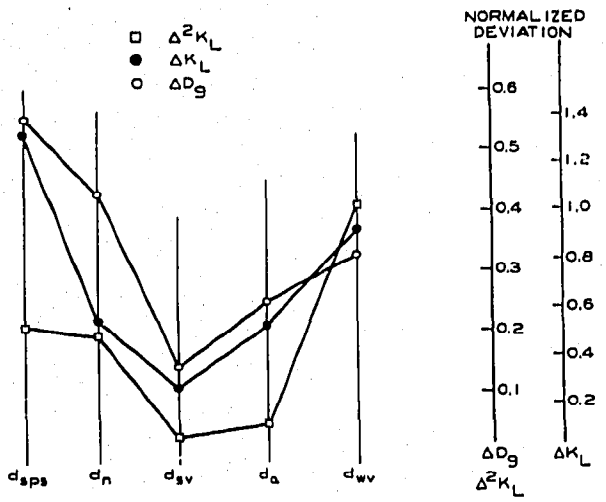

Fig. 5. Error analysis of diameter averages.

From this it can be seen that a log–log plot of $1/K_L$ *versus* d_p should have a slope of two. The slopes were calculated by least-squares analysis, and the results are shown in Fig. 5 as ΔK_L. Regardless of the slope, it should be the same for both solutes, *i.e.*, there should be no change in transfer mechanism. This analysis of error is shown in Fig. 5, abbreviated $\Delta^2 K_L$.

There was a minimum in the three measurements of consistency for the d_{sv} basis. This is not an unreasonable result since slow gel-phase diffusion should be best described by a volume averaged diameter.

Either d_{sps} or d_n is intuitively suggested by the random walk theories of eddy diffusion[13,14]. As shown in Fig. 6, there was a good linear correlation for both of these averages, except for the 70–80 mesh data. Different techniques were used for column packing in these runs, and it is reasonable that there is no agreement for these data.

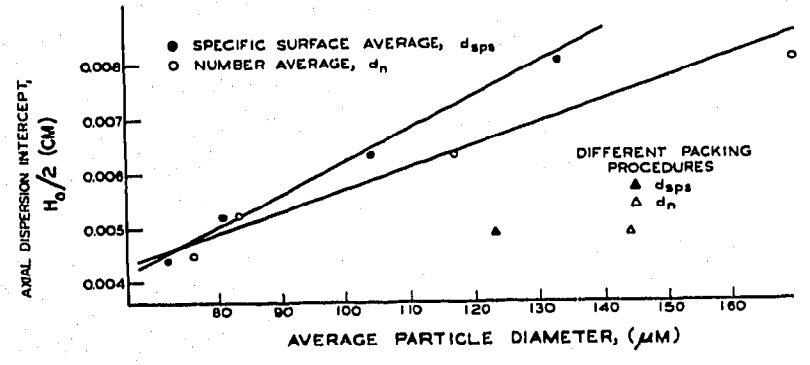

Fig. 6. Axial dispersion dependence on average particle diameter.

The regression parameters for the data shown in Fig. 6 are given in Table VI (excluding the 70–80 mesh data). The comparison is shown for the overall average eddy diffusion coefficient $<\lambda>$. The correlation coefficient is larger and the intercept is smaller for the d_{sps} line. There is better agreement between slope and $<\lambda>$ for d_{sps} than for d_n. From these comparisons, the conclusion is that the d_{sps} average gives a more consistent prediction of axial dispersion.

TABLE VI

DEPENDENCE OF AXIAL DISPERSION ON PARTICLE DIAMETER

	d_{sph} basis	d_n basis
Correlation coefficient[a]	0.998	0.991
Intercept[a]	3.5×10^{-4}	1.9×10^{-3}
Slope[a]	0.583	0.368
$<\lambda>$	0.620	0.557
$<\lambda>$ — slope	0.037	0.189

[a] Refers to data shown in Fig. 6.

Mass transfer

The dependence of mass transfer on particle diameter was given in eqn. (21). Theories dealing with slow film diffusion predict an exponent of 1 for d_p (ref. 8). Therefore, the slope of the log–log plot of $1/K_L$ *versus* d_p is a sensitive test for determining the controlling mechanism of mass transfer. The regression data in Table VII show that the slope is close to two in all cases, indicating that slow gel-phase diffusion was the controlling mechanism. The linearity of the relationships is an indication that there was not a change in the mechanism with variations in diameter.

TABLE VII

RELATION OF MASS TRANSFER COEFFICIENT TO PARTICLE DIAMETER

Condition	*Slope*[a]	*Intercept*	*Correlation coefficient*
15°, glucose	2.18	12.6	0.999
30°, glucose	1.92	11.0	0.984
45°, glucose	1.86	10.4	0.984
15°, raffinose	1.77	12.3	0.989
30°, raffinose	1.95	12.5	0.992
45°, raffinose	1.85	11.6	0.999

[a] Log $(1/K_L)$ *versus* log d_p.

The consistency of D_g can be seen from the data in Table VIII. There is good agreement except for some of the 100–120 mesh data at the higher temperatures. The slopes of the $H\alpha$ *versus* U plots were numerically small in these runs, making the calculations of D_g and K_L more susceptible to experimental error.

TABLE VIII

GEL-PHASE DIFFUSION COEFFICIENTS

Temperature (°C)	*Glucose ($D_g \times 10^7$)*			*Raffinose ($D_g \times 10^7$)*		
	100–120 mesh gel	*70–80 mesh gel*	*50–60 mesh gel*	*100–120 mesh gel*	*70–80 mesh gel*	*50–60 mesh gel*
15	3.13	3.02	2.85	1.00	1.04	1.01
30	4.82	5.25	3.73	1.72	1.79	1.14
45	6.40	7.84	7.03	3.02	2.85	2.97

Using the absolute rate theory of EYRING *et al.*[15], the activation energy of gel-phase solute diffusion can be calculated from the equation

$$\ln D_g = -E_a\left(\frac{1}{RT}\right) + \text{constant} \tag{22}$$

where D_g = calculated gel-phase diffusion coefficient, E_a = activation energy, R = gas constant, and T = absolute temperature.

The data shown in Table IX refer to solute behavior in the Bio-Gel P-2 systems. The activation energies increase in the expected way—with increasing molecular weight. All of the semilog plots of D_g *versus* $1/T$ were linear, confirming the conception of solute partitioning by localized restricted diffusion[16]. The activation energies are close to those reported for analogous gel systems, *cf.* 4.5–5.9 kcal/mole in ref. 17 and about 6.0 kcal/mole in ref. 18.

TABLE IX

VARIATION OF ACTIVATION ENERGY FOR DIFFUSION WITH SOLUTE

Solute	E_a *(kcal/mole)*
Glucose	5.34
Sucrose	5.90
Raffinose	6.50
Schardinger α-dextrin	6.53
Schardinger β-dextrin	6.73

Diffusivity retardation

The retardation ratio

$$\gamma = \frac{D_g}{D_m} \tag{23}$$

is useful in discussing the transport of solutes in gel systems. As shown in Table X, retardation is not sensitive to temperature. However, Tables X and XI show a high dependence of retardation on both solute and gel. There was a semilog correlation between the retardation ratio and solute molecular weight as shown in Fig. 7. It is of incidental interest that the intercepts of the lines in Fig. 7 agree only approximately with the equation of MACKEY *et al.*[19].

TABLE X

RETARDATION RATIOS, BIO-GEL P-2

	15°	*30°*	*45°*
Glucose	0.0587	0.0602	0.0671
Sucrose	0.0413	0.0492	0.0517
Raffinose	0.0307	0.0314	0.0429
Schardinger α-dextrin	0.0178	0.0263	0.0246
Schardinger β-dextrin	0.0145	0.0169	0.0210

TABLE XI

RETARDATION RATIOS, SEPHADEX GELS, 20°

	G-15	G-10
Glycine	—	0.0228
Glycerol	—	0.0266
Glucose	0.0717	0.0160
Sucrose	0.0376	0.0090
Raffinose	0.0297	0.0065
Schardinger α-dextrin	0.0122	0.0024

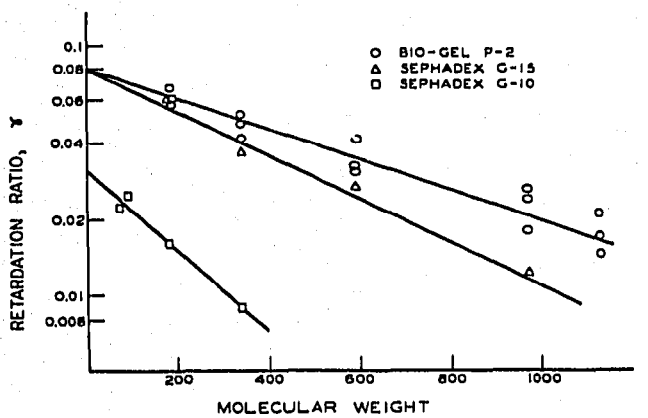

Fig. 7. Retardation ratio–molecular weight correlation.

$$\gamma = \frac{\varepsilon_g^2}{2 - \varepsilon_g} \tag{24}$$

based on a tortuosity model. The comparison is shown in Table XII.

TABLE XII

RETARDATION RATIOS PREDICTED BY THE RELATION OF MACKIE

	Predicted by eqn. (24)	*Measured intercept*
P-2	0.171	0.081
G-15	0.141	0.081
G-10	0.026	0.032

Solute partitioning was not found to be sensitive to flow rate or to any of the other experimental variables. The Sephadex gels were studied only at 20° so this conclusion cannot be completely generalized. All common colored materials (pH indicators, inks, Sephadex Blue Dextran 2000) were found to be chemically adsorbed on the Sephadex gels. Most of these materials were adsorbed on Bio-Gel P-2 with the exception of Na-Bromthymol Blue (Sargent) and Murexide (Polysciences). There was found to be an interaction between Schardinger α-dextrin and all of the Sephadex gels as shown in Table XIII by the abnormally large distribution coefficient for this solute.

TABLE XIII

EXPERIMENTAL DISTRIBUTION COEFFICIENTS

Solutes	*Gels*			
	P-2	*G-10*	*G-15*	*G-25*
Glycine	—	0.178	0.283	—
Glycerol	—	0.230	0.321	—
Glucose	0.410	0.186	0.287	0.361
Sucrose	0.361	0.136	0.241	0.328
Raffinose	0.291	0.082	0.179	0.287
Schardinger α-dextrin	0.271	0.119	0.289	0.371
Schardinger β-dextrin	0.243	—	—	—

There was found to be a good correlation between K_1 and molecular weight as shown in Fig. 8.

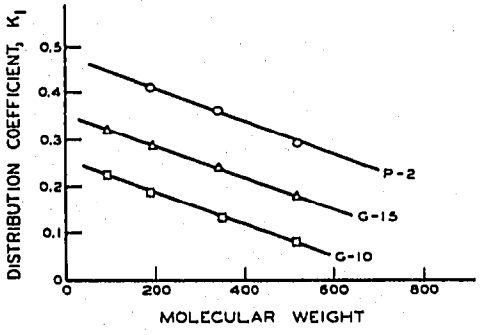

Fig. 8. Peak separation index correlation.

DISCUSSION AND CONCLUSIONS

Retardation of solute diffusivity in the gel matrix is the most important mechanism which causes band spreading in MSC systems. This is inherent in MSC since the same mechanisms are responsible for partitioning solutes according to molecular size. An interesting result of this relationship is that the bands which are eluted first from the column are spread less than subsequent bands. Since an excluded solute band does not involve gel phase transport, these bands are narrowest. This behavior was consistently observed and is shown in Table XIV for a representative series of curves.

TABLE XIV

REPRESENTATIVE SPREADING DATA

Solute	*Molecular weight*	*Distribution coefficient, K_1*	*Band spreading σ_v, (ml)*
Glucose	180	0.407	8.84
Sucrose	342	0.359	10.5
Raffinose	504	0.295	12.1
Schardinger α-dextrin	972	0.281	17.7
Schardinger β-dextrin	1,134	0.263	18.5
Dextran	12,000	0.0	2.94

This behavior agrees with observations in a polymer-related MSC system[20], but is contrary to the prediction of GIDDINGS[21].

Peak separation and band spreading are two effects which must be considered when designing a MSC separation. Two indices may prove useful in this respect,

$$I_{ps} = \frac{\Delta K_1}{\Delta \text{ molecular weight}} \tag{25}$$

$$I_{bs} = \frac{\Delta \log \gamma}{\Delta \text{ molecular weight}} \tag{26}$$

which are given in Table XV as calculated from data shown in Figs. 7 and 8. These indices are normalized measures of a gel's ability to separate molecules (I_{ps}) and of the increase in band spreading with increasing molecular weight (I_{bs}). As shown in Table XV, there is little difference between the abilities of the gels to separate molecules. However, the Sephadex gels caused more band spreading than did the Bio-Gel material. The reason for this is probably because the dextran matrix allowed more solute–gel interaction than did the acrylamide matrix. Thus, it would seem that the more inert a matrix is toward solutes, the better it will be in MSC applications.

TABLE XV

GEL EFFICIENCY PARAMETERS

I_{ps} = peak separation index; I_{bs} = band spreading index.

Gel type	$I_{ps} \times 10^4$	$I_{bs} \times 10^4$
P-2	3.65	6.07
G-15	3.54	8.67
G-10	3.50	15.9

ACKNOWLEDGEMENTS

The authors wish to thank R. W. NELSON and E. E. DICKEY for their help in evaluating and planning the thesis work, and KYLE WARD, Jr. and JOHN W. GREEN for their participation.

REFERENCES

1 A. J. P. MARTIN AND R. L. M. SYNGE, *Biochem. J.*, 35 (1941) 1358.
2 E. GLUECKAUF, *J. Chem. Soc.*, (1947) 1302.
3 E. GLUECKAUF, *Trans. Faraday Soc.*, 51 (1955) 34.
4 J. J. VAN DEEMTER, F. J. ZUIDERWEG AND A. KLINKENBERG, *Chem. Eng. Sci.*, 5 (1956) 271.
5 J. C. GIDDINGS AND K. L. MALLIK, *Anal. Chem.*, 38 (1966) 997.
6 S. T. SIE AND G. W. A. RIJNDERS, *Anal. Chim. Acta*, 38 (1967) 3.
7 W. W. YAU AND C. P. MALONE, *J. Polymer Sci., Part B*, 5 (1967) 663.
8 P. B. HAMILTON, D. C. BOGUE AND R. A. ANDERSON, *Anal. Chem.*, 32 (1960) 1782.
9 N. P. POVEY, *Doctor's Dissertation*, The Institute of Paper Chemistry, Appleton, Wisc., 1969, 117 pp.

10 K. W. PEPPER, D. REICHENBERG AND D. K. HALE, *J. Chem. Soc.*, (1952) 3129.
11 J. HAPPEL AND H. BRENNER, *Low Reynolds Number Hydrodynamics*, Prentice-Hall, New York, 1965, 553 pp.
12 H. PURNELL, *Gas Chromatography*, Wiley, New York, 1962, p. 94.
13 J. C. GIDDINGS, *Dynamics of Chromatography*, Vol. 1, M. Dekker, New York, 1965, 323 pp.
14 F. HELFFERICH, *Ion Exchange*, McGraw-Hill, New York, 1962, 624 pp.
15 S. GLASSTONE, K. J. LAIDER AND H. EYRING, *The Theory of Rate Processes*, McGraw-Hill, New York, 1941, 875 pp.
16 P. FLODIN, *Dextran Gels and Their Application in Gel Filtration*, Pharmacia, Uppsala, Sweden, 1962, 85 pp.
17 S. B. HOROWITZ AND I. R. FENICHEL, *J. Phys. Chem.*, 68 (1964) 3378.
18 P. SPACEK AND M. KUBIN, *J. Polymer Sci., Part C*, 16 (1967) 705.
19 J. S. MACKIE AND P. MEARES, *Proc. Roy. Soc. (London), Ser. A*, 232 (1955) 489.
20 L. H. TUNG, J. C. MOORE AND G. W. KNIGHT, *J. Appl. Polymer Sci.*, 10 (1966) 1261.
21 J. C. GIDDINGS, *Anal. Chem.*, 39 (1967) 1027.